Flash Boiling Spray of Diesel Fuel Mixed with Ethane and Its Effects on Premixed Diesel Combustion

Y. Kobashi[1]*, S. Hirako[2], A. Matsumoto[2], K. Naganuma[2]

[1] Division of Energy and Environmental Systems, Graduate School of Engineering, Hokkaido University, Japan

[2] Department of Mechanical Engineering, Kanazawa Institute of Technology, Japan

Abstract

Mixtures of gaseous and liquid fuels have the potential to induce flash boiling under in-cylinder conditions close to the top dead center, something that can be expected to be suitable for a premixed diesel combustion that demands a way to enhance lean mixture formation. The present study mixes ethane, which is a natural gas component, into diesel fuel as ethane has a high vapor pressure that facilitates flash boiling and as ethane has a low cetane number that prolongs the ignition delay. This paper investigates spray characteristics of a diesel fuel – ethane mixture, and the engine performance and exhaust emissions are evaluated in a single cylinder engine. The test results show that the flash boiling enhances the lean mixture formation, and realizes combustion with low soot and low NOx without EGR (exhaust gas recirculation) while also improving thermal efficiency. An additional test was performed to identify the effects of the flash boiling and the ignition delay, and the results show that the long ignition delay plays the

* Corresponding author at: Kita 13, Nishi 8, Kita-ku, Sapporo, Hokkaido, Japan
E-mail address: kobashi@eng.hokudai.ac.jp (Y. Kobashi)

most important role in the thermal efficiency and emission changes and that the flash boiling facilitates the formation of leaner mixtures that lower the overall combustion rate and achieves very low NO_x emissions.

Keywords: Flash Boiling, Premixed Diesel Combustion, Ethane, Mixed Fuel, Emissions

Nomenclature:

$dp/d\theta_{max}$	Maximum pressure rise rate [MPa/deg.CA]
$dQ/d\theta$	apparent heat release rate [J/deg.CA]
ΔP_{sat}	difference between the pressure on bubble point curve and the in-cylinder pressure [MPa]
p_{inj}	fuel injection pressure [MPa]
Q_{1st}: Q_{2nd}	ratio of first and second injection quantities
V_{et}	volume fraction of ethane in the mixed fuels [vol.%]
z	distance from injection nozzle [mm]

Greek symbol:

η_i	indicated thermal efficiency [%]
ρ_a	ambient density [kg/m^3]
θ_{inj}	signal incident timing of fuel injection (single injection case) [deg.CA ATDC]
$\theta_{inj.1st}$	signal incident timing of first fuel injection [deg.CA ATDC]
$\theta_{inj.2nd}$	signal incident timing of second fuel injection [deg.CA ATDC]
τ_{ign}	ignition delay defined as the period from the injection signal incidence until the start of the main combustion

1. Introduction

In modern diesel engines employing premixed diesel combustion, high-pressure fuel injection with advanced timings would promote atomization and facilitate the leaner mixture formation, and exhaust gas recirculation (EGR) has been used to lengthen ignition delays and to ensure the formation of the premixed mixture in diesel combustion [1-2]. Despite these advantages, earlier timings of fuel injection with high pressures increase the unburned emissions due to the fuel reaching the squish area in the combustion chamber [3], and high EGR rates make it difficult to control the intake oxygen concentration in transient operation due to the slowness of the response.

Gasoline-fueled compression ignition engines have attracted increasing attention [4-6], since the low reactivity and high volatility of gasoline are suitable qualities characteristics to enhance lean mixture formation. Manente et al. demonstrated 57% indicated thermal efficiency in a single cylinder heavy duty with the gasoline-fueled compression ignition [7]. In this strategy, however, the ignition timing control for a wide range of operating conditions is still challenging as commonly-available gasoline is too resistant to auto-ignition. To make the operation

67 easier while retaining the advantage of the lean mixture formation, won et al. proposed
68 the use of blends of gasoline and diesel fuel [8], since it is preferable to have fuels with
69 a better reactivity than those of gasoline, and it is practical to blend those
70 commercially-available fuels. Researchers at University of Birmingham applied the
71 blends of gasoline and diesel fuel as well, and the mixing fractions were optimized to
72 improve the premixed diesel combustion [9-10].

73 Prior to this attracting attention, researchers at Doshisha University proposed
74 that the use of mixed fuels consisting of a high volatility fuel with low reactivity (such
75 as gasoline and gaseous fuels) and a high reactivity fuel with low volatility (such as
76 diesel fuel) would make it possible to obtain better characteristics of evaporation and
77 control of the ignition timing [11]. In addition to the above benefits, they suggested that
78 the high volatility fuel induces flash boiling when the fuel is discharged into a
79 combustion chamber with lower pressure than its saturation pressure [12]. Following
80 Senda, Wada et al. [13-14] applied mixed fuels consisting of *i*-pentane (C_5H_{12}) and
81 *n*-tridecane ($C_{13}H_{28}$) to a premixed charge compression ignition engine with very early
82 injection. Anitescu et al. visualized the flash boiling sprays of the blends of gasoline and
83 diesel fuel, injected into ambient air [15]. However, there have been only a few studies
84 addressing a flashing spray injected into engine-relevant conditions near top dead center.

As one of them, the previous paper by the authors introduced a flashing spray in the premixed diesel combustion with late injections [16]. Gaseous fuel, ethane was used to achieve the flash boiling even near top dead center, and it was mixed into diesel fuel to ensure successful compression ignition. Another study reported the results in the literature [12], where liquid petroleum gas (LPG) was mixed into *n*-tridecane ($C_{13}H_{28}$), and the mixed fuel was introduced into the conventional diesel combustion with late injections while heating the fuel to ensure the flash boiling conditions. Both the studies reported the improvements of the efficiency and the emissions with the flashing sprays. However, the characteristics of the flash boiling spray injected into an engine-relevant high ambient density conditions were not examined, and the mechanism that improved the combustion was not figured out.

In the present paper, the spray characteristics of the diesel - ethane mixed fuel were investigated at a variety of mixing fractions. Engine tests were performed while introducing the flashing spray into the premixed diesel combustion, and data analysis was carried out to clarify the combustion improvement mechanism and to isolate the effects of the flash boiling and the ignition delay on the engine performance and the exhaust emissions.

2. Experimental Setup and Conditions

2.1 Fuels tested

The fuels mainly tested here are mixtures of ethane and JIS No.2 diesel fuel in a variety of mixing fractions. The properties of the tested fuels are detailed in Table 1. The JIS No.2 Diesel fuel has a high boiling point and high reactivity, and ethane has a low boiling point and the octane number of 108. A pressure-temperature diagram of the diesel fuel – ethane mixed fuel, calculated with SUPERTRAPP (NIST), is shown in Fig.1. Diesel fuel consists of multiple components, and it was replaced by *n*-tridecane ($C_{13}H_{28}$) in the calculations. With increasing ethane fraction, V_{et} shifts the saturated liquid curve to higher pressures, and it can be expected that the flash boiling will take place at the in-cylinder pressure with a high fraction of ethane. The present study employed the difference between the pressure on the saturated liquid curve and the ambient pressure, termed ΔPsat, to express the degree of the flash boiling. A part of these experiments use a mixed fuel consisting of *i*-octane and Shellsol (MC421) to distinguish the effects of the flash boiling and the ignition delay as Shellsol is mainly composed of large isoparaffins with high distillation temperatures and low cetane numbers, and a mixed fuel of this kind would not induce flash boiling in the engine cylinder. The mixed-in fraction of Shellsol was determined to match the ignition timing with the mixed fuel of ethane and diesel fuel.

[Table 1]

[Fig.1]

2.2 Fuel supply system

Figure 2 shows a diagram of the fuel supply system. To maintain ethane in the liquid phase during introduction into the fuel supply system, a bladder accumulator (at ② in Fig.2) pressurized with nitrogen was used and the pressure in the flow path of ethane was maintained above the vapor pressure. When the flow path was filled with ethane, the ethane was introduced into the mixing tank (at ① in Fig.2) where diesel fuel was already accumulated, and the mixture of ethane and diesel fuel was agitated at 600 rpm for 30 minutes. Then the mixed fuel was transferred to the double-acting cylinder (③) facilitated by the intensifier (④) to be compressed to the injection pressure of 40 MPa.

[Fig.2]

2.3 Spray visualization in a constant volume vessel

The spray was visualized in a constant volume vessel with shadowgraph photography. The vessel equips with two quartz glass windows lying in the same optical

path line. The diameter and thickness of the quartz glasses are 120 mm and 45 mm, respectively, and 90 mm in diameter is available as a field of view. A fuel injector with a single hole nozzle (0.1 mm in diameter) was attached at the top of the vessel.

The arrangement for the shadowgraph photography is schematically shown in Fig.3. A xenon lamp was used as the light source with a plano-convex lens (100 mm diameter, 1000 mm focal length) which collimates the light, and the collimated light passing through the vessel was focused on a lens of a high-speed video camera (SA1.1, Photron) with the second plano-convex lens (100 mm diameter, 1000 mm focal length). The spray images were taken with the recording rate of 30000 frames per second (fps), and the light intensity was adjusted with an ND filter. The spatial resolution for this setup was 0.072 μm/pixel.

The analysis began while subtracting a background image without the injection from spray images, in order to eliminate the background noise. An intensity threshold level which was used to separate the spray region from the background ambient gas was carefully determined with the as-recorded spray images of V_{et} = 60 % as this fuel was most volatile, and it was most difficult to separate the spray region. Pixels with intensity levels below the threshold were defined as the spray region, and the spay angles were measured. The spray tip penetration was measured with the ensemble-averaged images.

155 The experimental conditions are detailed in Table 2. The vessel was filled with
156 the 0.90 MPa CO_2 at the room temperature to achieve the engine-relevant ambient
157 density of 16.1 kg/m^3. The fuel was injected from a single hole 0.10 mm diameter
158 nozzle. The pressure in the vessel was lower than the in-cylinder pressure, and ΔP_{sat} in
159 the spray experiment was positive when the ethane fraction, V_{et} was above 30 vol.%. All
160 the ΔPsat detailed in Table 2 were calculated assuming the fuel temperature of 300 K in
161 Fig.1.

162 **[Figure 3]**

163 **[Table 2]**

164 2.4 Engine test

165 The specifications of the single cylinder diesel engine used in the present study
166 are detailed in Table 3. The single cylinder diesel engine equips with a toroidal type
167 combustion chamber. The bore and stroke are 83 and 85 mm, the displacement volume
168 is 460 cc, and the compression ratio is 19.3. The fuel injection system introduced in
169 Fig.2 was used, and a 10 hole nozzle with the nominal hole diameters of 0.101 mm was
170 employed. The experimental conditions are detailed in Table 4. The engine rotation
171 speed was maintained constant at 1000 rpm. The mixed-in fraction was varied as an

172 experimental parameter while adjusting the fuel flow rate to maintain the constant heat
173 supply of 400 J/cycle. As the primary purpose of the present paper is to investigation the
174 relation between the spray characteristics of the diesel fuel – ethane mixed fuel and the
175 characteristics of the premixed diesel combustion, the engine tests were performed at
176 the constant rotation speed and engine load. The variations of these experimental
177 parameters were not tested but should be examined in future work.

178 Table 5 provides the accuracy and the detection limit of measurements. The
179 soot concentration was measured with a smoke meter (AVL, 415S). As the accuracy is
180 unknown, the detectable limit is detailed in Table 5. The exhaust gas concentrations of
181 CO, CO_2 and NO_x were measured with an FT-IR exhaust gas analyzer (HORIBA,
182 MEXA-6000FT), and THC emissions were measured with an FID analyzer (HORIBA,
183 MEXA-1170HFID). The accuracy of all the gas concentrations was within ±1% FSO.
184 The in-cylinder pressures were measured with a pressure transducer (Kistler, 6125C)
185 which has accuracy better than ±0.4% of full scale output (FSO), while a charge
186 amplifier (Kistler, 5010B) was used to convert the charge signal from the pressure
187 transducer into an output voltage. Unlike the experiments where repetition of
188 measurements is possible, so that an error analysis is performed, as in Ref. [17] dealing
189 with a hybrid cooling-drying system, it is difficult for engine tests to repeat many tests

190 at each operating point due to the many data points involved, and in engine tests,
191 cycle-by-cycle variations in the combustion processes may cause a significant error and
192 deteriorate the accuracy of measurements. In the present study, to mitigate the effects of
193 the cycle-by-cycle variations, the data obtained in the experimental conditions where the
194 coefficients of variance of indicated mean effective pressure (IMEP) were less than 3%
195 were used for the evaluation, except for some data in Fig.10. The profiles of the
196 in-cylinder pressure were recorded for 120 cycles, and the averaged pressure was
197 employed to calculate the apparent heat release rate. The exhaust gas concentrations
198 were measured for 30 seconds, and the averaged values were adopted.

199 **[Table 3]**

200 **[Table 4]**

201 **[Table 5]**

202 **3. Results and Discussion**

203 3.1 Spray Characteristics of the Diesel Fuel – Ethane Mixed Fuels

204 Figure 4 shows the spray shape near the nozzle for different volume fractions
205 of ethane, V_{et}. The sprays with positive ΔP_{sat} which may possibly induce flash boiling,
206 disperse in the radial direction directly at the nozzle exit (top of figure) as the fuel flow

207 containing bubbles formed in the nozzle expands immediately after the discharge. The
208 temporal changes of the whole spray images are shown in Fig.5, clearly showing that
209 the spray width increased with V_{et}. The flash boiling phenomenon enhances the liquid
210 atomization and vaporization and the formation of droplets, promoting the dispersion
211 further in the downstream direction, due to the turbulent motion.

212 **[Fig.4]**

213 **[Fig.5]**

214 The spray cone angles and the spray angles are shown in Fig.6. The spray cone
215 angle was defined based on the spray width at z = 5 mm with the shadowgraph images
216 enlarging the region close to the nozzle, and the whole spray images were used to define
217 the spray angle based on the maximum spray width from z = 25 mm to 38 mm. Using
218 10 sets of the frames, the averaged angles as well as the extent of the fluctuation were
219 calculated. By considering the spatial resolution 0.072 μm/pixel, the resolution of the
220 spray cone angle measured at z = 5 mm is 0.80 degree/pixel, and that of the spray angle
221 measured at z = 32 mm is 0.13 degree/pixel. Taking into account the resolution and the
222 extent of the data fluctuation, both these angles clearly increase with increasing V_{et}. The
223 spray cone angle is more sensitive to V_{et} than the spray angle, as the initial spray
224 dispersion is strongly affected by the flow during the passage of the nozzle (by the

225 bubbles growth due to the phase-change) and the spray dispersion further downstream is
226 affected by the turbulent motion of the surrounding gas.

227 In Fig.7, the relationships between the ΔP_{sat} and the spray angle are plotted
228 against the various ambient densities, ρ_a. The open symbols are the data from the
229 previous study using a heated mixed fuel of *n*-tridecane and *i*-pentane (Wada et al.,
230 2007) and the solid symbols are the data obtained in this study. It is difficult to compare
231 the data from the present and the previous study directly due to the differences in the
232 definition of the spray angle, while it is possible to compare the gradient against the
233 ΔP_{sat}. The previous study showed that the effect of the flash boiling on the spray
234 dispersion was less pronounced at the high ambient density conditions, while the
235 present data showed that the spray angle increased evenly with increasing ΔP_{sat} at all
236 the ambient densities here, likely as the diesel fuel – ethane mixed fuel has the higher
237 ΔP_{sat}. Suggesting that a more pronounced effect of flash boiling can be expected by
238 using the diesel fuel – ethane mixed fuel in the engine test, which will be reported
239 below.

240 **[Fig.6]**

241 **[Fig.7]**

242 A plot of the spray tip penetration with the diesel fuel – ethane mixed fuel is

243 shown in Fig.8. The initial spray tip penetrations are largely proportional to the time
244 from the start of injection also with the flash boiling, likely as the dense region in the
245 center of the spray is maintained. At around 0.15 ms after the start of injection, the spray
246 tip penetration is proportional to the square-root of the time, implying that the exchange
247 of momentum between the spray and the surrounding gas has become active. At this
248 point, the part of the fuels with a large ethane fraction lose momentum faster due to the
249 flash boiling effect.

250 **[Fig.8]**

251 3.2 Effects of the Ethane Fraction on Engine Performance and Exhaust Gas Emissions

252 Figure 9 shows the profiles of the in-cylinder pressure, p and the apparent heat
253 release rate, $dQ/d\theta$ at the time of the fuel injection signal, θ_{inj} at -4 deg.CA ATDC.
254 Considering that the delay in arrival of the injection signal from the actual injection is
255 approximately 4 deg.CA, the diesel fuel auto-ignited immediately after the start of the
256 actual injection. With increasing ethane fraction, V_{et}, the ignition delay increased, and
257 the low temperature heat release (LTHR) which is typically observed in premixed
258 combustion appears prior to the main combustion of V_{et} = 50 vol.%. At this θ_{inj}, it was
259 difficult to establish the combustion with the coefficient of variance of indicated mean

effective pressure (IMEP) less than 5% with V_{et} = 60 and 65 vol.% due to the long ignition delay.

[Fig.9]

Figure 10 shows the variations of the indicated thermal efficiency, η_i and the maximum pressure rise rate, $dp/d\theta_{max}$ with V_{et} and θ_{inj}. The indicated thermal efficiency decreased with increasing V_{et} from 0 to 50 vol.% as the longer ignition delay retarded the combustion and decreased the degree of constant volume. The early injection timing was expected to advance the combustion phase and improve the degree of constant volume, however it deteriorated the indicated thermal efficiency due to the increased cooling loss, and additionally the advanced injection was limited by the very large increase in $dp/d\theta_{max}$. With V_{et} at 60 and 65 vol.%, a better indicated thermal efficiency was obtained with the earlier injection timing around -25 deg.CA ATDC. The longer ignition delays and the flash boiling with these fuel mixtures enabled the formation of leaner mixture combustion that lowered the flame temperature. However, further advances in the injection deteriorated the η_i due to the formation of an excessively lean mixture while retarding the injection deteriorated the η_i, due to the excessively late combustion phase.

[Fig.10]

278 To further identify the advantages of the diesel fuel - ethane mixed fuels more
279 specifically, the best (optimum) injection timings, those which resulted in the best
280 indicated thermal efficiencies were selected, and the profiles of the optimum apparent
281 heat release rates, $dQ/d\theta$ are shown in Fig.11. The optimum combustion phase with V_{et}
282 = 0, 30 and 50 vol.% was later than that of the V_{et} of 60 and 65 vol.% possibly as the
283 flame temperatures of the V_{et} = 0, 30, and 50 vol.% may be higher and the later
284 combustion resulted in a reduced cooling loss. The leaner mixture of V_{et} = 60 and 65
285 vol.% formed by the longer ignition delays and the flash boiling may lower the flame
286 temperatures, so that advancing the combustion phase and avoiding the cooling loss
287 made the increase in the degree of constant volume possible.

288 **[Fig.11]**

289 Figure 12 shows the changes in ΔP_{sat} and the ignition delays, τ_{ign}, with the V_{et}
290 at the best injection timings, where τ_{ign} was defined as the period from the injection
291 signal arrival until the start of the main combustion. The τ_{ign} was maintained nearly
292 constant up to when the ratio of the less reactive ethane was high (note that 50 vol.% is
293 equal to 73 mol.%) as also reported previously [11], but a further increase of V_{et} above
294 60 vol.% increased τ_{ign} strongly, because of the low content of the more reactive diesel
295 fuel component. Due to the high vapor pressure as well as the early injection

296 accompanied by the long ignition delay, ΔP_{sat} with V_{et} = 60 and 65 vol.% was positive,
297 and a large spray dispersion would be as could be expected.

298 **[Fig.12]**

299 The changes in the maximum pressure rise rate, $dp/d\theta_{max}$ and the exhaust
300 emissions with V_{et} are shown in Fig.13, and the changes in the indicated thermal
301 efficiency, η_i and its related factors are shown in Fig.14. The cooling loss, ϕ_{cool} is
302 calculated as:

303 $$\phi_{cool} = \eta_{comb} - \eta_i/\eta_{th}\eta_{glh} \quad (1)$$

304 where η_{comb} is the combustion efficiency, η_{th} is the thermal efficiency of theoretical
305 Otto-cycle, and η_{glh} is the degree of constant volume burning [18].

306 From V_{et} = 0 to 50 vol.%, the best η_i decreased, and $dp/d\theta_{max}$ increased. It
307 appears that with increasing V_{et}, the air-fuel mixture became leaner and closer to
308 stoichiometric, increasing the flame temperature and causing the simultaneous ignition
309 at multiple locations. The further increase in the V_{et} up to 60 and 65 % increased the
310 best η_i and decreased the $dp/d\theta_{max}$. Here, it would appear that the leaner mixtures
311 formed by the flash boiling and the long ignition delay decreased the flame temperature
312 and reduced the cooling loss while lowering the overall combustion rate even with the
313 earlier combustion. The above discussion of the flame temperature was supported by the

changes in the cooling loss, ϕ_{cool}, where the cooling loss increased from V_{et} = 0 to 50 vol.%, and decreased from V_{et} = 50 to 65 vol.%.

NO_x increased from V_{et} = 0 to 50 vol.%, and decreased from V_{et} = 50 to 65 vol.%. No significant soot was detected in the present experiments, and the soot decreased with increasing V_{et}. As the result, combustion without soot and without NO_x was accomplished with V_{et} = 65 vol.%. One drawback here was the increases of THC and CO and the decrease of the combustion efficiency, η_{comb} as the formation of the leaner mixture and the decrease in the flame temperature tend to increase the unburned emissions due to the quenching. This combustion inefficiency had a negative effect on the thermal efficiency, but the reduction in the cooling loss overcame this negative change as well as the slight increase in the degree of constant volume burning, η_{glh}.

[Fig.13]

[Fig.14]

3.3 Isolation of the Effects of Ignition Delay and Flash Boiling

To isolate the effects of the ignition delay and the flash boiling, the mixed fuel of Shellsol (MC421) and *i*-octane was tested, adjusting the amount of *i*-octane to match the ignition delay of the diesel fuel – ethane mixed fuel (V_{et} = 60 vol.%). The profiles of the

331 in-cylinder pressure, p and the apparent heat release rate, $dQ/d\theta$ are shown in Fig.15.
332 There was a discrepancy in the timings of the LTHR, and the onset of the high
333 temperature heat release of the Shellsol – *i*-octane mixed fuel was earlier with 0.5
334 deg.CA compared to that of the diesel fuel – ethane mixed fuel. The difference may
335 cause no significant effect on this comparison. The rate of heat release of the diesel fuel
336 – ethane mixed fuel was lower than the Shellsol – *i*-octane mixed fuel even with the
337 same ignition delay, likely as the leaner mixture could reduce the overall combustion
338 rate in combination with the improvement in $dp/d\theta_{max}$ of 0.3 MPa/deg.CA.

339 **[Fig.15]**

340 The indicated thermal efficiency, η_i, the combustion efficiency, η_{comb}, the
341 cooling loss, ϕ_{cool}, and NO_x emissions are plotted for the two mixed fuels in Fig.15.
342 There were no significant differences in the η_i, the η_{comb}, and the ϕ_{cool}, and the η_i of the
343 Shellsol – *i*-octane mixed fuel exceeded 40%. It was evident that the indicated thermal
344 efficiency strongly depends on the ignition delay. It was not possible to determine the
345 effect on the soot emission as no soot was detected in this condition. From the fact that
346 the diesel fuel – ethane mixed fuel resulted in lower NO_x emissions, it appears that the
347 air-fuel mixture of the diesel fuel – ethane mixed fuel was leaner and its flame
348 temperature was lower.

As the result, it may be concluded that the ignition delay plays the most important role in the efficiency and in the emission characteristics, and that the flash boiling enhances the leaner air-fuel mixture formation that lowers the overall combustion rate and the NO_x emissions further.

[Fig.16]

4. Conclusions

The present study introduced mixed fuels of diesel fuel and ethane in premixed diesel combustion, aiming to utilize its flash boiling and ignition delay characteristics. The spray characteristics of the mixed fuels were investigated in a constant volume vessel, and the engine performance and the emissions were evaluated at the IMEP around 0.35 MPa in a single cylinder engine. The conclusions may be summarized as follows:

1. The high pressure on the bubble point curve of the diesel-fuel – ethane mixed fuel induces the flash boiling even in the in-cylinder condition close to the top dead center, expands the spray width right at the nozzle exit and disperses the spray in the downstream region even at the high ambient density.
2. The ethane fraction more than 60 vol.% is needed to gain the ignition delay which

allows the early injection accompanied by the flash boiling and achieved the low temperature combustion conditions.

3. The long ignition delay of the diesel fuel – ethane mixed fuel plays a major role in improving the thermal efficiency, and the flash boiling makes the air – fuel mixture more homogeneous, reducing NO_x emissions.

4. The major drawback of the diesel fuel – ethane mixed fuel is the complex fuel supply system. This may be suitable for stationary engines.

References

[1] Akihama, K., Takatori, Y., Inagaki, K., Sasaki, S. and Dean, A. M., “Mechanism of Smokeless Rich Diesel Combustion by Reducing Temperature”, SAE Technical Paper, No. 2001-01-0655, 2001.

[2] Ogawa, H., Li, T., and Miyamoto, N., “Characteristics of Low Temperature and Low Oxygen Diesel Combustion with Ultra-high Exhaust Gas Recirculation”, International Journal of Engine Research, Vol.8, Issue 4, pp.365-378, 2007.

[3] Ogawa, H., Xiong, Q., Obe, T., Sakane, Y., and Shibata, G., “Improvements in Thermal Efficiency of Premixed Diesel Combustion with Optimization of Combustion-Related Parameters and Fuel Volatilities”, International Journal of Engine Research, Vol.16, Issue 1, pp.81-91, 2015.

[4] Kalghatgi, G., Risberg, P., and Ångström, H., "Advantages of Fuels with High Resistance to Auto-ignition in Late-injection, Low-temperature, Compression Ignition Combustion", SAE Technical Paper 2006-01-3385, 2006.

[5] Kalghatgi, G., Risberg, P., and Ångström, H., "Partially Pre-Mixed Auto-Ignition of Gasoline to Attain Low Smoke and Low NOx at High Load in a Compression Ignition Engine and Comparison with a Diesel Fuel", SAE Technical Paper 2007-01-0006, 2007.

[6] Hanson, R., Splitter, D., and Reitz, R., “Operating a Heavy-Duty Direct Injection

393 Compression-Ignition Engine with Gasoline for Low Emissions", SAE Technical
394 Paper 2009-01-1442, 2009.
395 [7] Manente, V., Johansson, B., and Cannella, W., "Gasoline Partially Premixed
396 Combustion, the Future of Internal Combustion Engines?", International Journal of
397 Engine Research, Vol.12, Issue 3, pp.194-208, 2011.
398 [8] Won, H. W., Pitsch, H., Tait, N. and Kalghatgi, G., "Some Effects of Gasoline and
399 Diesel Mixtures on Partially Premixed Combustion and Comparison with the
400 Practical fuels Gasoline and Diesel in a Compression Ignition Engine", Journal of
401 Automotive Engineering, Vol.226, Issue 9, pp.1259-1270, 2012.
402 [9] Zhang, F., Xu, H., Rezaei, S. Z., Kalghatgi, G. and Shuai, S.-J., "Combustion and
403 Emission Characteristics of a PCCI Engine Fuelled with Dieseline", SAE Technical
404 Paper 2012-01-1138, 2012.
405 [10] Zhang, F., Rezaei, S. Z., Xu, H. and Shuai, S.-J., "Experimental Investigation of
406 Different Blends of Diesel and Gasoline (Diseline) in a CI Engine", SAE Int. J.
407 Engines 7(4), pp.1920-1930, 2014.
408 [11] Senda, J., Kawano, D., Hotta, I., Kawakami, K., and Fujimoto, H., "Fuel Design
409 Concept for Low Emission in Engine Systems", SAE Technical Paper 2000-01-1258,
410 2000.
411 [12] Senda, J., Wada, Y., Kawano, D., and Fujimoto, H., "Improvement of Combustion
412 and Emissions in Diesel Engines by Means of Enhanced Mixture Formation Based
413 on Flash Boiling of Mixed Fuel", International Journal of Engine Research, Vol.9,
414 Issue 1, pp.15-27, 2008.
415 [13] Wada, Y., Nishimura, Y., Yamaguchi, A., Magara, N. et al., "Controlling PCCI
416 Combustion with Mixed Fuel - Application of Flashing Spray to Early Injection",
417 SAE Technical Paper 2007-01-0624, 2007.
418 [14] Wada, Y., Nishimura, Y., Yamaguchi, A., Magara, N., Senda, J., and Fujimoto, H.,
419 "Combustion Control in DI Compression Ignition Engine with Partially Premixed
420 Charge Operation Using Flashing Spray of Mixed Fuel", International Conference
421 on Modeling and Diagnostics for Advanced Engine Systems (COMODIA), Sapporo,
422 2008.
423 [15] Anitescu, G., Bruno, T. J., and Tavlarides, L. L., "Dieseline for Supercritical
424 Injection and Combustion in Compression-Ignition Engines: Volatility, Phase
425 Transitions, Spray/Jet Structure, and Thermal Stability", Energy and Fuels, 26(10),
426 PP.6247-6258, 2012.
427 [16] Matsumoto, A., Kobashi, Y., Kato, S., Naganuma, K., Ito, T., Kawakita, S.,
428 Morishima, S., and Kondo, W., "Flash Boiling Effect of Ethane Mixed Fuel on

Pre-mixed Diesel Combustion", Transactions of Society of Automotive Engineers of Japan (in Japanese), Vol.48, Issue 4, pp.795-800, 2017.
[17] Acar, M. S. and Arslan, O., "Performance Analysis of a New Hybrid Cooling – Drying System", Environmental Progress & Sustainable Energy, https://doi.org/10.1002/ep.12832.
[18] Shudo, T., Nabetani, S. and Nakajima, Y., "Analysis of the Degree of Constant Volume and Cooling Loss in a Spark Ignition Engine Fuelled with Hydrogen", International Journal of Engine Research, Vol.2, Issue 1, pp.81-92, 2001.

Table 1 Properties of the tested fuels

	Ethane	Diesel fuel	Shellsol MC421	*i*-octane
Carbon number	C2	C10 – 26	C11.2	C8
Lower calorific value [MJ/kg]	47.3	43.1	44.0	44.4
Density [kg/m^3]	340*	820	774	690
Boiling point [ºC]	-89	200 - 350	185 - 199	99
Ignition point [ºC]	515	250	417	411

* at 293 K, 4 MPa (calculate with SUPERTRAPP)

Table 2 Experimental conditions in the constant volume vessel

Volume fraction of ethane, V_{et}	[%]	0	30	50	60
Pressure difference in flash boiling, ΔP_{sat}	[MPa]	-0.9	1.2	2.2	2.5
Injection pressure, p_{inj}	[MPa]	40			
Injection period	[ms]	2			
Nozzle hole diameter	[mm]	0.10			
Ambient pressure, p_a	[MPa]	0.90			
Ambient temperature, T_a	[K]	293			
Ambient density, ρ_a	[kg/m^3]	16.3			
Ambient gas		CO_2			

Table 3 Specifications of the single cylinder diesel engine

Displacement	[cm^3]	460
Bore	[mm]	83
Stroke	[mm]	85
Geometric compression ratio		19.3 : 1
Combustion chamber shape		Toroidal type
Fueling system		Direct injection
Configurations of injection nozzle		hole dia.: 0.101 mm number of holes: 10

Table 4 Experimental conditions in the single cylinder diesel engine

Engine rotation speed [rpm]	1000
Injection pressure, p_{inj} [MPa]	40
Timing of injection signaltiming, θ_{inj} [deg.CA ATDC]	-30 to 1
Fuel energy supplied [J/cycle]	400
Indicated mean effective pressure [MPa]	around 0.35
Air intake condition	Natural aspiration (No EGR or boost)

Table 5 Accuracy of measurements

Measurements	Accuracy
CO	±50 ppm
CO_2	±0.05 vol.%
NO_x	±10 ppm
THC	±50 ppm
Smoke	0.02 mg/m^3 (detection limit)
In-cylinder pressure	±0.04 MPa

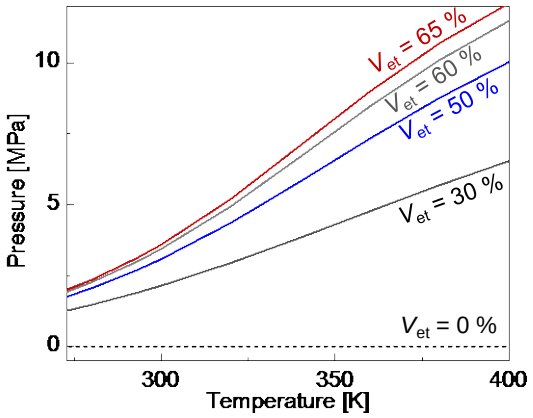

Figure 1 Pressure-temperature diagram of the C_2H_6 – n-$C_{13}H_{28}$ mixed fuels with various mixing fractions of ethane, V_{et}

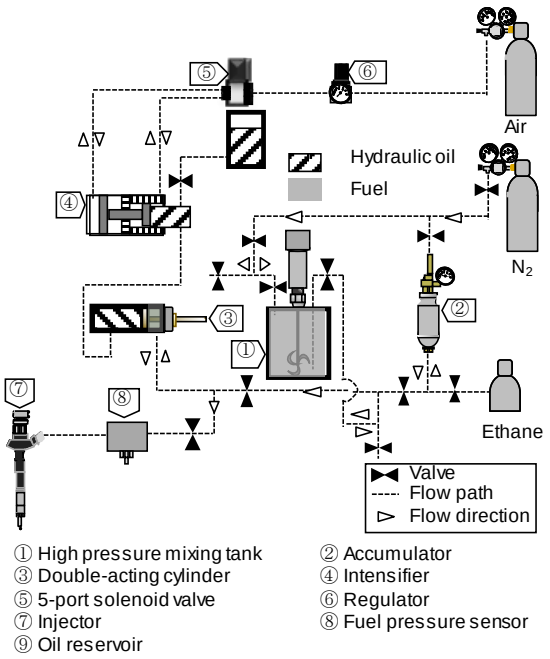

Figure 2 Schematic of the fuel supply system including the fuel mixing and the pressure parts

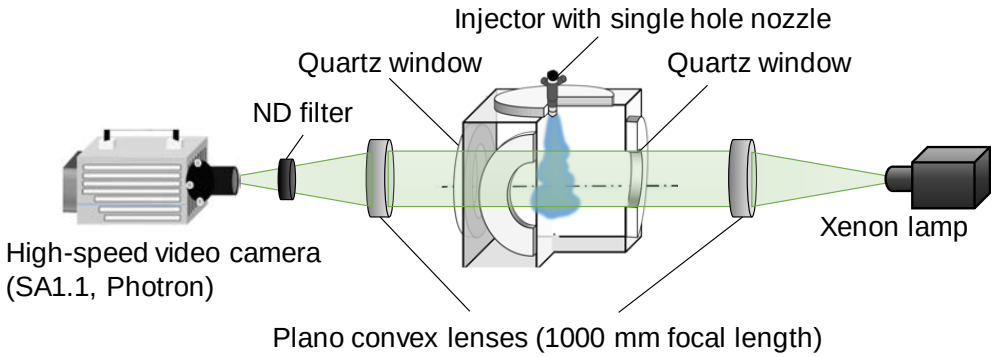

Figure 3　Optical setup for shadowgraph photography

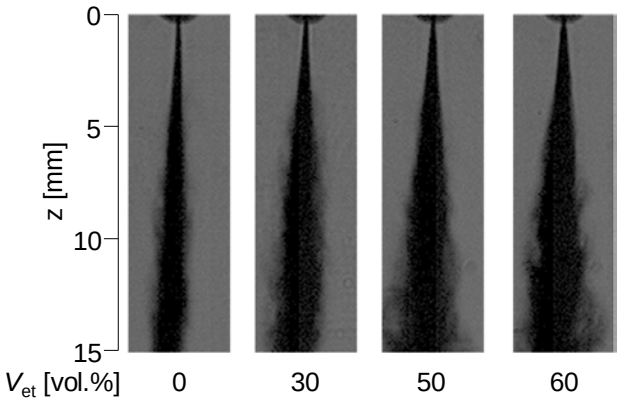

Figure 4　Changes in spray shape near the nozzle exit (top of panels) with ethane fraction, V_{et}

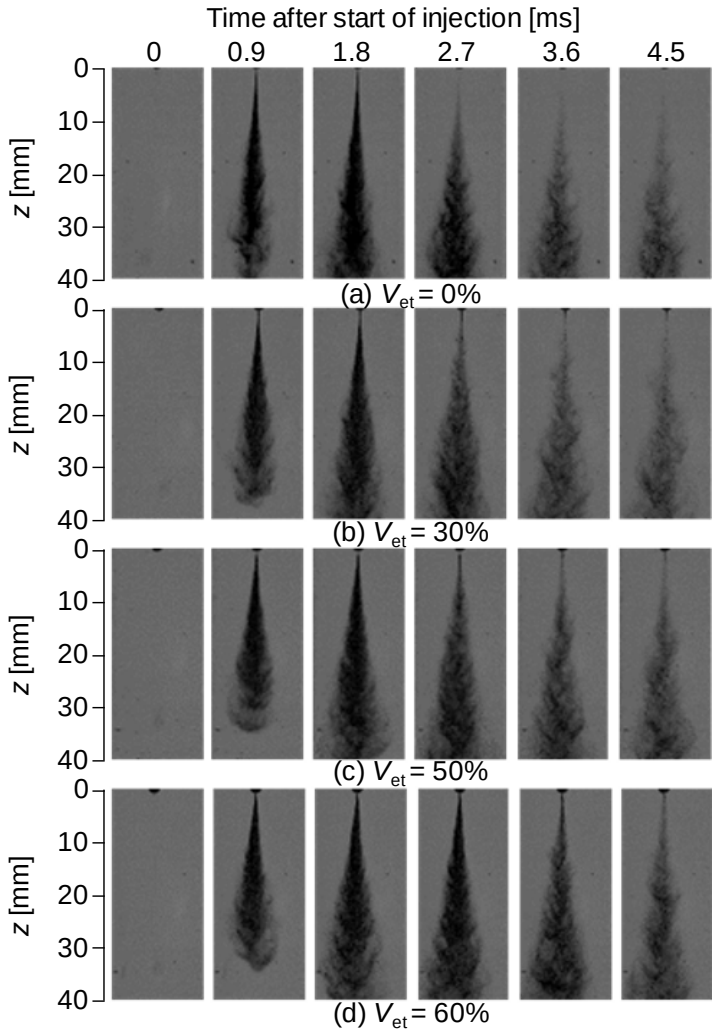

Figure 5 Temporal changes in spray shapes with the ethane fraction, V_{et}

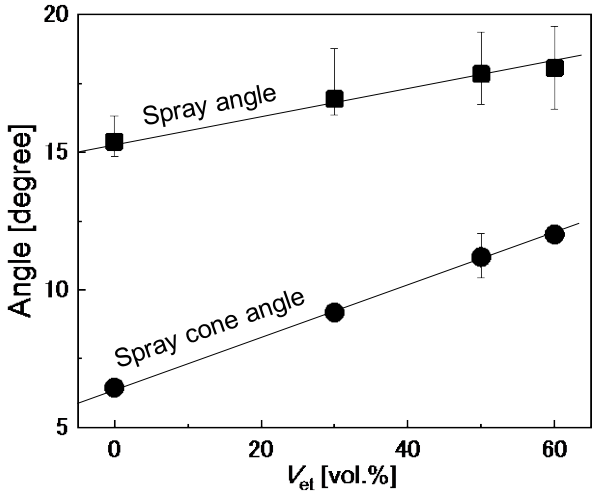

Figure 6 Changes in spray cone angle and spray angle with the ethane fraction, V_{et}

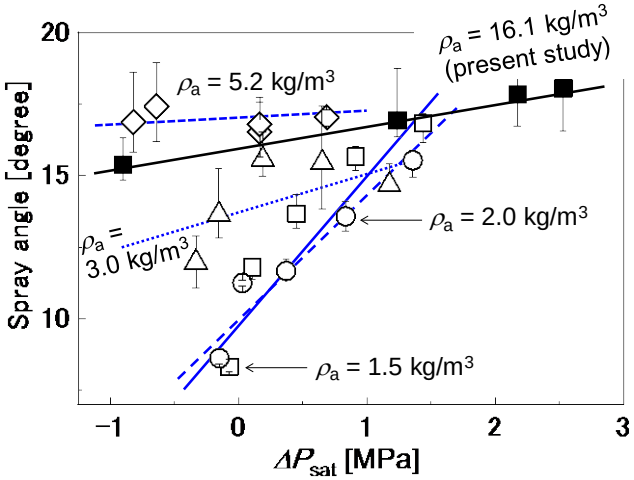

Figure 7 Relation between ΔP_{sat} and the spray angle at various ambient densities, ρ_a
Open symbols: previous study (Wada et al., 2007)
Solid symbol: present study

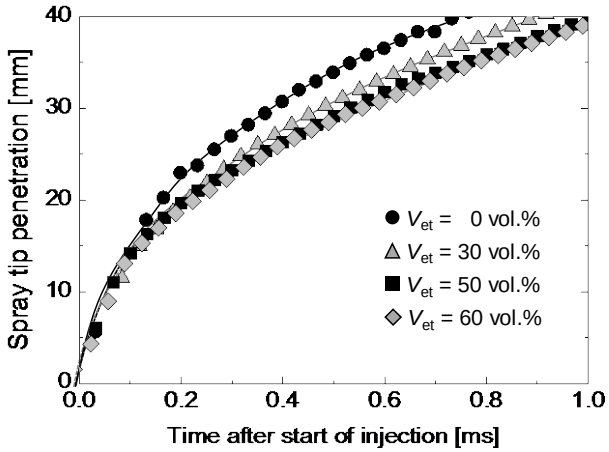

Figure 8 Plot of spray tip penetrations for different ethane fractions, V_{et}

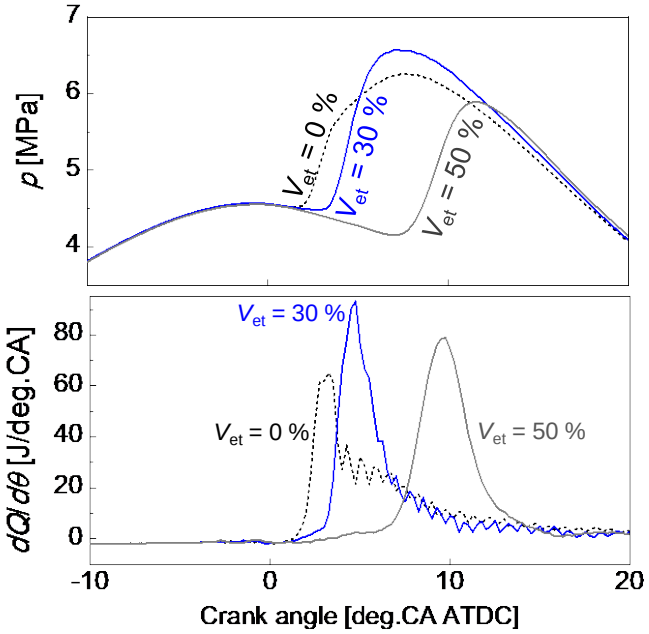

Figure 9 Profiles of in-cylinder pressures, p and apparent heat release rates, $dQ/d\theta$ at the injection timing, θ_{inj} of -4 deg.CA ATDC

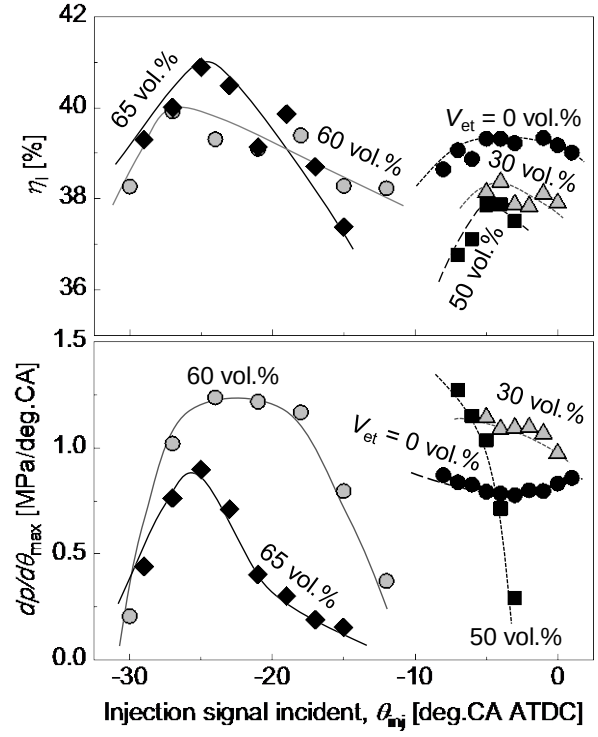

Figure 10 Variations in indicated thermal efficiency, η_i and maximum pressure rise rate, $dp/d\theta_{max}$ with the injection signal incident timing, θ_{inj} and the ethane fraction, V_{et}

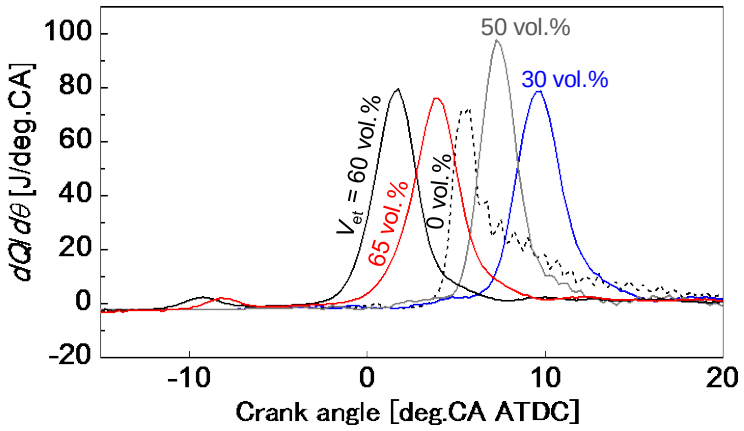

Figure 11 Profiles of the apparent heat release rate, $dQ/d\theta$ at the optimum injection timings

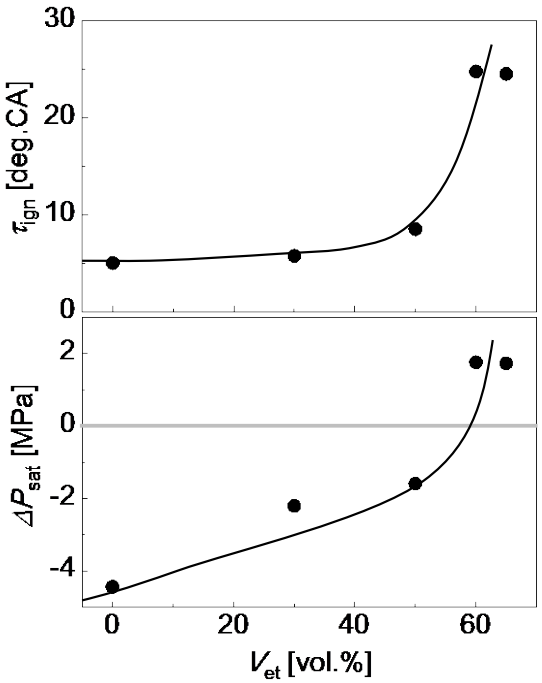

Figure 12 Plots of the ignition delays, τ_{ign} and differences between the in-cylinder pressure and pressure on the bubble point curve, ΔP_{sat} versus ethane fraction, V_{et} at the optimun injection timings

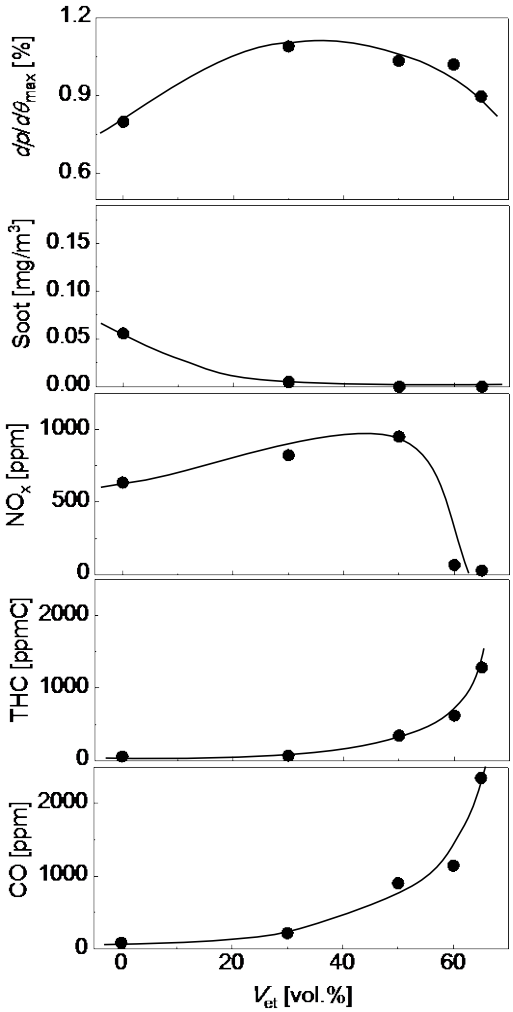

Figure 13 Changes in maximum pressure rise rate, $dp/d\theta_{max}$ and exhaust gas emissions with ethane fraction, V_{et} at the optimum injection timing

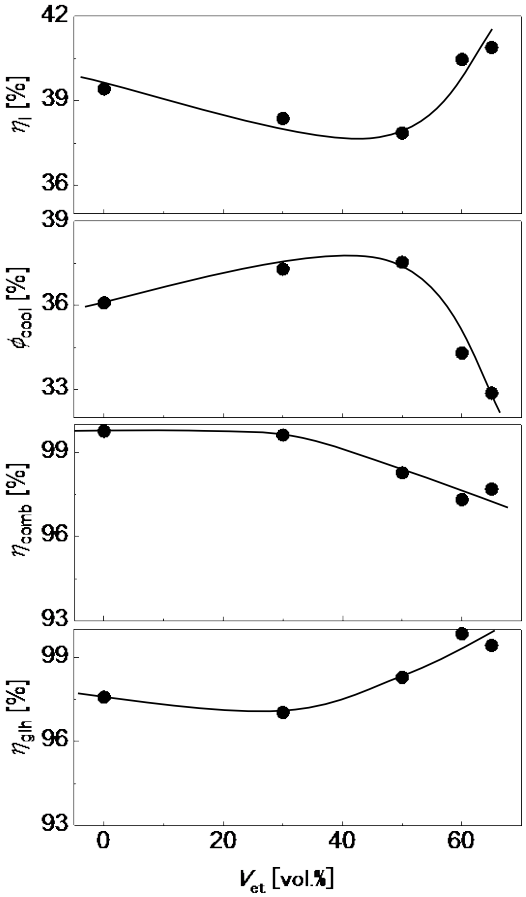

Figure 14 Changes in indicated thermal efficiency, η_i and its related factors, cooling loss, ϕ_{cool}; combustion efficiency, η_{comb}; and degree of constant volume burning, η_{glh} with ethane fraction, V_{et} at the optimum injection timing

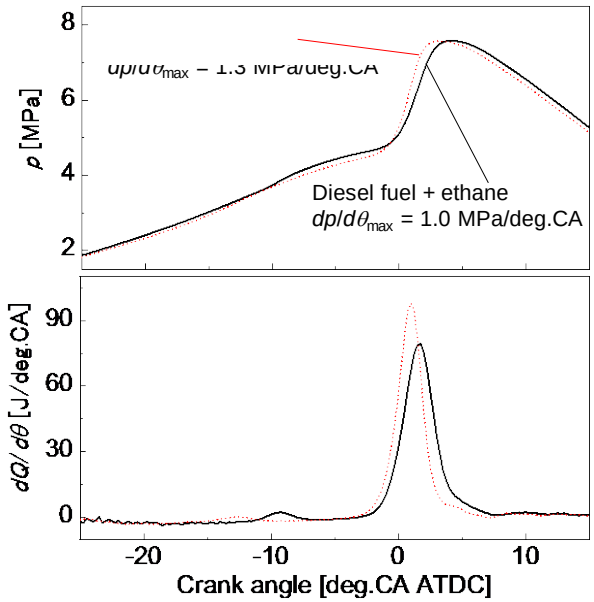

Figure 15 Plot of in-cylinder pressure, p and apparent heat release rate, $dQ/d\theta$ for the mixed fuels of Diesel fuel – ethane and Shellsol – *i*-octane (θ_{inj} = -27 deg.CA ATDC)

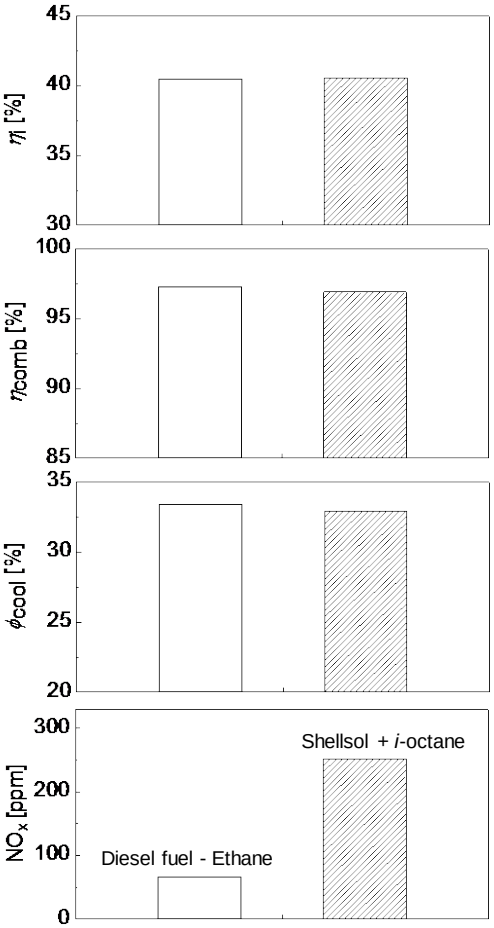

Figure 16 Details of the indicated thermal efficiency, η_i, combustion efficiency, η_{comb}, cooling loss, ϕ_{cool}, and NO_x emissions of the fuel mixtures of Diesel fuel – ethane and Shellsol – *i*-octane (θ_{inj} = -27 deg.CA ATDC)